NPS73-88-001

NAVAL POSTGRADUATE SCHOOL

Monterey, California

ON THE RESISTANCE OF CERAMICS TO HIGH VELOCITY PENETRATION

J. STERNBERG

JULY 1988

Prepared for:
Naval Postgraduate School
Monterey, CA 93943-5000

NAVAL POSTGRADUATE SCHOOL
Monterey, California

Rear Admiral R. C. Austin
Superintendent

K. T. Marshall
Acting Provost

This report was prepared by:

Unclassified
Security Classification of this page

REPORT DOCUMENTATION PAGE

1a Report Security Classification: Unclassified	1b Restrictive Markings
2a Security Classification Authority	3 Distribution Availability of Report: Approved for public release; distribution is unlimited.
2b Declassification/Downgrading Schedule	
4 Performing Organization Report Number(s)	5 Monitoring Organization Report Number(s)
6a Name of Performing Organization: Naval Postgraduate School; 6b Office Symbol (If Applicable): 73	7a Name of Monitoring Organization: Naval Postgraduate School
6c Address (city, state, and ZIP code): Monterey, CA 93943-5000	7b Address (city, state, and ZIP code): Monterey, CA 93943-5000
8a Name of Funding/Sponsoring Organization: Naval Postgraduate School; 8b Office Symbol (If Applicable):	9 Procurement Instrument Identification Number: O&MN, Direct Funding
8c Address (city, state, and ZIP code): Monterey, CA 93943	10 Source of Funding Numbers: Program Element Number; Project No; Task No; Work Unit Accession No

11 Title (Include Security Classification): On the resistance of ceramics to high velocity penetration

12 Personal Author(s): Joseph Sternberg

13a Type of Report	13b Time Covered	14 Date of Report (year, month,day)	15 Page Count
Research Report	From To	June 1988	44

16 Supplementary Notation: The views expressed in this thesis are those of the author and do not reflect the official policy or position of the Department of Defense or the U.S. Government.

17 Cosati Codes			18 Subject Terms (continue on reverse if necessary and identify by block number)
Field	Group	Subgroup	High Velocity Penetration, Ceramic Armor

19 Abstract (continue on reverse if necessary and identify by block number

It is known that high velocity penetration for ductile materials can be represented analytically by a modified hydrodynamic theory. The strength term for the target corresponds to the pressure required to expand a cavity, if the dynamic yield strength is substituted for the static yield strength. Indentation pressures are closely related to the cavity expansion pressures. In this paper it is shown that the key parameters for indentation in brittle materials are similar to but not identical to those for ductile materials. The strength terms for ceramics as measured in ballistic tests are much lower than would be predicted on the basis of the indentation measurements. It is found that the ratio of the target strength term to hardness increases as the fracture toughness of the targets increases. The findings on penetration resistance are used together with cavity expansion theory to estimate the relative size of the craters in ceramic targets.

20 Distribution/Availability of Abstract	21 Abstract Security Classification	
[X] unclassified/unlimited [ ] same as report [ ] DTIC users	Unclassified	
22a Name of Responsible Individual: Joseph Sternberg	22b Telephone (Include Area code): (408) 646-3496	22c Office Symbol: 73

DD FORM 1473, 84 MAR 83 APR edition may be used until exhausted
All other editions are obsolete

security classification of this page
Unclassified

ABSTRACT

It is known that high velocity penetration for ductile materials can be represented analytically by a modified hydrodynamic theory. The strength term for the target corresponds to the pressure required to expand a cavity, if the dynamic yield strength is substituted for the static yield strength. Indentation pressures are closely related to the cavity expansion pressures. In this paper it is shown that the key parameters for indentation in brittle materials are similar to but not identical to those for ductile materials. The strength terms for ceramics as measured in ballistic tests are much lower than would be predicted on the basis of the indentation measurements. It is found that the ratio of the target strength term to hardness increases as the fracture toughness of the targets increases. The findings on penetration resistance are used together with cavity expansion theory to estimate the relative size of the craters in ceramic targets.

TABLE OF CONTENTS

I. INTRODUCTION.

Various materials have been considered as possible substitutes for steel as components of armor against kinetic energy projectiles. Some ceramics provide a combination of extreme hardness and low density thereby offering the potential of reducing the weight per unit area required for a given level of protection. But while penetration in metal targets has been extensively studied, the effectiveness of ceramics in resisting penetration is much less well understood. Target fracture under high velocity impact is a major complication which prevents the use of monolithic designs. The purpose of this paper is to identify those mechanical properties of ceramics that provide improved resistance to penetration, recognizing fracture of the target as an important consideration, and to establish how those properties relate to target damage in the vicinity of the penetration. Implicit in the use of ceramics for armor are substantial new armor design problems.

There is also interest in the possible use of ceramics for armor protection at impact velocities above 1.5 km/sec., the limit of current battlefield launchers. Much higher launcher velocities may be achievable with electromagnetic launchers or other new techniques under development. For high density tungsten rods striking steel targets, increasing the impact velocity from 1.5 km/sec to 2.5 km/sec doubles the penetration of long rods as the strength of the target becomes unimportant compared to the impact pressures. [1] By a velocity of 4 km/sec. the hydrodynamic limit for penetration is being approached asymptotically. On the other hand it may require velocities well over 4 km/sec. to reach the point where the strength of ceramic targets no longer matters.

At the present state of knowledge, theoretical methods that can be applied to the problem of kinetic energy impact in ceramics are limited. Hydrocodes have been successfully developed for the computation of penetration in metal targets. But the

behavior of ceramics under dynamic impact is highly complex and it isn't clear how to account for the state of target fracture and how to represent the constitutive relations for ceramics above the elastic limit in the hydrocodes. Alternatively, a number of authors have had considerable success with analytical representations for penetration in metals and other materials in which a single strength term for the target, (and a strength term for the penetrator) have been added to the hydrodynamic representation of impact. [2-4] The larger the value of the strength parameter for the target, the better the resistance of the target to penetration in the velocity region below the hydrodynamic limit. The value of this strength parameter is often taken as constant, although there is not any theoretical reason why it should necessarily be independent of impact velocity.

Tate [4] proposed that the magnitude of the target strength term, and therefore the resistance to penetration, primarily depends on the flow stress that must be reached to overcome the elastic forces in the target material. Other authors [3,5] have argued that the resistance to penetration primarily depends on the resistance of the target material to deformation as it is forced out of the way. If the latter is the correct interpretation, then the shear strength of the target above the elastic limit would be a key parameter. Many ceramics appear to suffer a major loss of shear strength above the elastic limit. [6]

The magnitude of the strength term used in such a modified hydrodynamic theory for ceramics should presumably reflect the effect of target fracture. Observations of projectile impacts on brittle targets show that fracture propagates into the target at high speeds. [7] Consequently, except for the initial instant of impact, penetration in brittle materials is likely to mean penetration in a fractured target. If the target is not strongly confined, the resistance to penetration will be markedly reduced. [8] One important question is whether the extent of target fracture significantly affects penetration resistance even when the target is confined.

Experiments show that as the impact velocity is increased the extent of target fracture increases. Therefore we might anticipate a decrease in the appropriate value of the target strength parameter to be used as impact velocity is increased. Such a trend would not necessarily continue indefinitely. At high enough impact velocities, depending on the material, the velocity at which the interface between the penetrator and the target penetrates the target would exceed the elastic wave velocity in the target. Since the velocity of fracture in brittle materials is a substantial fraction of, but is less than, the elastic wave velocity, general fracture of the target ahead of the penetrator would not then occur. However at such high impact velocities the target strength term in the equation would make a negligible contribution to the resistance to penetration. In the velocity range of interest for this paper the target strength term should be important and might well vary to some degree with velocity.

Another question is the size of the crater produced by penetration of ceramic targets. In ductile materials, the crater volume is found to scale inversely with the Brinell hardness of the target and directly with the energy of the penetrator. [9] What should control the size of craters in ceramic targets?

I will explore these questions by an analysis of data from indentation measurements, material properties derived by the exposure of ceramics to strong shock waves, and data available from ballistic firings against ceramic targets. The analysis of indentation measurements in ceramics is a key step in reaching this objective. As noted by Tate, the pressure required for quasi-static penetration in metals provides a basis for estimating the magnitude of the target strength term for high velocity impact. That leads to the investigation of the relationship between indentation measurements in ceramics and the results of ballistic experiments.

The ballistic data on ceramics that will be used in this paper come from the work of Donaldson et al where an analytic theory was developed to fit penetration data obtained with tungsten carbide spheres. [5] There are differences between this analytical representation and that used by previous authors. Accordingly, in the following section, I will briefly compare the assumptions made by different authors in deriving modified hydrodynamic integral theories for kinetic energy (and shaped charge) penetration. This will be followed by an examination of indentation measurements and indentation theory for ductile and brittle materials which is a necessary preliminary for the interpretation of measured values of the strength term in high velocity impact in ceramics.

II. MODIFIED HYDRODYNAMIC THEORIES.

Hydrodynamic theory provides a satisfactory description of the performance of shaped charges, where the velocities are generally so high that the pressures generated greatly exceed material strengths. The velocity variation along the shaped charge jet is gradual so that at any instant a steady state description can be used for the interaction region of the jet and the target. Let the velocity U represent the rate at which the interface is penetrating into the target and let V represent the jet velocity relative to the target. If both target and penetrator behaved as incompressible fluids, Bernouilli's equation for the pressure in the target and the pressure in the jet on the axis at the interface would give

$$\rho_j \frac{(V-U)^2}{2} = \rho_t \frac{U^2}{2}$$

where ρ_j is the density of the jet and ρ_t is the density of the target. Eichelberger [10] introduced an additional pressure term in this basic equation for shaped charge penetration to make the right hand side of the equation read

$$\rho_t \frac{U^2}{2} + \sigma$$

where the quantity σ "will be presumed to be the difference between two quantities, σ_t and σ_j, which represent the resistance of the target and the jet, respectively, to the plastic deformation required by the penetration process." But in the case of shaped charges, the strength of the target material and jet, and therefore this new term, only become significant when the jet velocity has fallen to relatively low values and jet penetration is near its end.

As noted previously, integral theories for long rod penetration have been developed using similar modifications to the hydrodynamic theory. Tate [4] represented the pressure on the axis at the interface as

$$p = \frac{1}{2}\rho_t U^2 + R_t = \frac{1}{2}\rho_p (V-U)^2 + Y_p \qquad (1)$$

The terms R_t and Y_p were identified as the strength terms for the target and penetrator materials respectively. Since the target material must be moved out of the way of the penetrator, pressures in the target must be high enough so that a large volume of the target material is above the elastic limit. That requires a value of R_t much larger than the dynamic flow stress. This geometrical constraint was considered to be analogous to what had been found in static punching of metals where the pressure required for penetration was several times the yield stress. [11]

In equation 1, ρ_t, and ρ_p are constant and it is assumed that once in motion the penetrator and target materials behave as frictionless incompressible fluids (i.e. perfect fluids). The forces are purely pressure forces and there is no resistance to the distortion of fluid elements. If the target is a highly compressible material, such as some plastics, penetration will be less than that predicted by incompressible theory. [12] For most of the

materials used in heavy armor and armor penetrators, the incompressible representation appears adequate.

In principle, where the target material retains strength after it is set in motion, the flow of such a material could not conform to that of a "perfect fluid". The fluid elements always undergo distortion in perfect fluid flows and if the target material retains a shear strength, plastic work must be done on the target material. This work will appear predominantly as heat, in effect, introducing a dissipative term into the flow. Higher pressure (i.e. higher velocity) would then be required to produce the same rate of penetration. Wright [13] examined the general form of the terms that would have to be added to equation 1 to account for the shear stresses in rigid/plastic materials but the terms themselves were not evaluated. Where the target loses all of its shear strength after it is set in motion, it still may not be appropriate to represent the flow of the target material as a "perfect fluid". In some ceramics, the target appears to be turned into rubble as it is set in motion. [14] The flow of the resulting irregular granular "fluid" under compression may be strongly dissipative. Further work is needed to clarify whether or not these departures from "perfect fluid" flow significantly alter the prediction of penetration.

Tate used his theory to fit long rod penetration experiments in metals and some plastics. An alternate form of a modified hydrodynamic theory was later used by Donaldson et al [5] to fit penetration data using tungsten carbide spheres (instead of long rods) which produced shallow penetrations of the targets. The deceleration force on a penetrating nondeforming sphere was represented by [8]

$$F = A\left(C\rho_t \frac{U^2}{2}\right) + \rho_t E_* \qquad (2)$$

where A is the projected area of the penetrator surface in contact with the target, and C is a constant. (It was assumed that the flow field in the target could be represented by the

Newtonian flow approximation applicable to aerodynamic flows at hypersonic speeds. [15] A value of 1/2 was chosen for the constant C in order to provide the best fit to a range of experiments. E_* was regarded as a characteristic property of the target material representing the amount of energy per unit mass absorbed by the target during deformation. A detailed review of the work of the Aeronautical Research Associates of Princeton (ARAP) including the interpretation of E_* is contained in Ref. 16.

It is evident that the mathematical representation for the pressure on the axis at the penetrator/target interface is of the same form as that used by Tate (and other authors) where the pressures in the target are represented by a dynamic term, proportional to U^2, plus a target strength term.) The product $\rho_t E_*$ can be readily recognized as holding the same place in this representation as R_t for Tate's formulation. The absolute values of $\rho_t E_*$ determined by fitting the non-deforming sphere experiments obviously depend on the specific equation, constants, and flow field assumption used to represent penetrator deceleration. Thus, as discussed in Ref. 16, the basic condition for the application of Newtonian theory is not satisfied for hypervelocity impact. Nevertheless, since the same equation has been used to fit all of the experimental data, I will assume that the experiments with tungsten carbide spheres provide a measure of the relative values of $\rho_t E_*$ for the different materials tested. Results obtained in the following section for impact in steel indicate that the absolute values of $\rho_t E_*$ are reasonable as well.

III. INDENTATION IN DUCTILE AND BRITTLE MATERIALS

A. Metals.

The pressure needed to slowly expand a cavity in the target material provides a surprisingly good analogy for the target strength term in high velocity impact if dynamic properties of the target are substituted for quasi-static properties. [4] The theory for the expansion of a spherical cavity in a ductile target was developed many years ago by Hill.

[17] Surrounding the cavity in cavity expansion is an extensive region of plastic flow which grows in proportion to the size of the cavity. For metals, the volume of the plastic flow region is from 100-200 times as large as the volume of the cavity. The pressure required for expansion depends on the yield stress as well as other mechanical properties of the target and is given by

$$\frac{p}{Y} = \frac{2}{3} + \frac{2}{3}\ln\left(\frac{E}{3(1-\nu)Y}\right) \tag{3}$$

where ν is Poisson's ratio and E is Young's modulus. While the pressure required for penetration is primarily fixed by the yield strength of the target material, the shear behavior of the target material above the elastic limit also affects the required penetration force. If the material strain hardens, the required pressure is increased above that shown in equation 3. Using the expansion theory as an analogy for high velocity impact, the target strength term is identified with the cavity expansion pressure. The target strength term therefore has the same theoretical dependence on target yield strength and mechanical properties as the expansion pressure in the cavity expansion theory, except that the dynamic yield strength of the target must be substituted for the quasi-static yield strength measured in tensile tests.

A point of interest is a theoretical solution for the dynamic expansion of a cavity developed by Hopkins. [18] To simplify the solution, the assumptions were made that the material behaved as a non work-hardening elastic/plastic material (so the effect of shear stresses in the material in motion are included) and that it was elastically incompressible; i.e. $\nu = \frac{1}{2}$. For expansion at a steady velocity, the pressure required for cavity expansion was found to be the sum of Hill's quasi-static solution and a dynamic term equal to $\frac{3}{2}\rho_t U_s^2$ (where U_s is the cavity surface velocity). Consequently the form of the equation for p is similar to that of equation 1. However, the radial "flow field" of this solution represented by the dynamic terms is not an appropriate approximation to the "flow field" in

high velocity penetration where the target material that has been set in motion flows around the penetrator rather than flowing radially from the penetrator.

As will be discussed, the pressure required for indentation in ductile materials, theoretically, is closely related to the pressure required for cavity expansion for a significant range of material properties. Consequently standard laboratory hardness measurements should provide a simple way to assess the magnitude of the strength term in high velocity impact. In addition, as has been noted, there are major similarities between the indentation behavior of metals and the indentation behavior of brittle materials which suggests that indentation measurements should also be useful in predicting the magnitude of the strength term for ceramic targets. First I will review the state of theory and experiment for indentation in metals.

Two quite different penetration modes are found in indentation measurements in metals. In one mode, displaced plastic material flows towards the surface as penetration proceeds. Outside the plastic region, the remainder of the target is effectively rigid, and elasticity of the target does not play any role in the solution. The slip-line theory for a rigid-plastic material has been used to theoretically represent this behavior. [17] The pressure required for penetration depends on the force required to overcome the shear forces in the plastic material as it flows so that the shear strength above the elastic limit directly influences the predicted force.

In the second penetration mode, instead of flowing toward the surface, the target material is pushed out in a roughly radial direction as penetration occurs. Elasticity of the target plays a direct role in that the elastic compression of the target must be sufficient to accommodate the volume of the cavity created. The elastic field in the target must be determined in order to obtain a solution for the penetration force. The penetration pressure is primarily determined by the yield strength Y and Young's modulus E.

Which penetration mode occurs depends on the elastic properties and yield strength of the target, and the bluntness of the indenter. It is to be expected that the mode of flow found would correspond to the least work for penetration of the indenter. For a relatively blunt indenter, such as a Vicker's pyramid indenter which has an included angle of 136°, if the stiffness of the material is increased without limit, $E \rightarrow \infty$, then at some point the target material behaves as a rigid-plastic material and the displaced material flows towards the surface. Alternatively, if the target material properties are held constant and the bluntness of the indenter is varied, the pressure required to move the material around the indenter to the surface increases as the bluntness of the indenter increases and we might expect a transition to the subsidence mode when some high bluntness is reached. Since the free surface is always present, the transition from one penetration mode to the other is not likely to be sharp and mixed flow modes are probable.

Hill's theory for the expansion of a spherical cavity in a target (equation 3) has been used as the basis for representing the subsidence penetration mode. However, in order to obtain close agreement between theory and experiment, the spherical cavity theory has to be modified to account for both the effect of the free surface and the non-spherical region in the vicinity of the penetrator on the resulting stress field in the target. Marsh [19] showed that the Vicker's hardness measurements (the Vicker's hardness H is the ratio of the penetration force to the indentation area and so is the penetration pressure) for a range of materials including various metals and plastics could be fit by a solution of the same form as the spherical cavity theory, but with different constants. Marsh represented the ratio of the pressure H required for indentation to the yield strength Y by an expression of the form

$$\frac{H}{Y} = A + B \ln Z \qquad (4)$$

for lnZ less than 4.3, where the parameter Z is approximately equal to $(3/(4+\nu))E/Y$. The constants A and B were set equal to .28 and .60 respectively. Hill's spherical expansion

theory and Marsh's correlation for indentation measurements are compared in Fig. 1. The ratio H/Y is less than the ratio p/Y for the expansion of a spherical cavity, ranging from .86 of the spherical cavity result at lnZ = 2 to .88 of the spherical cavity result at lnZ = 4.0. Marsh attributed the smaller values of H/Y to the reduced constraint provided by the free surface. For deep penetration the effect of the free surface should disappear and the pressure for penetration might be expected to increase from Marsh's correlation to Hill's theory.

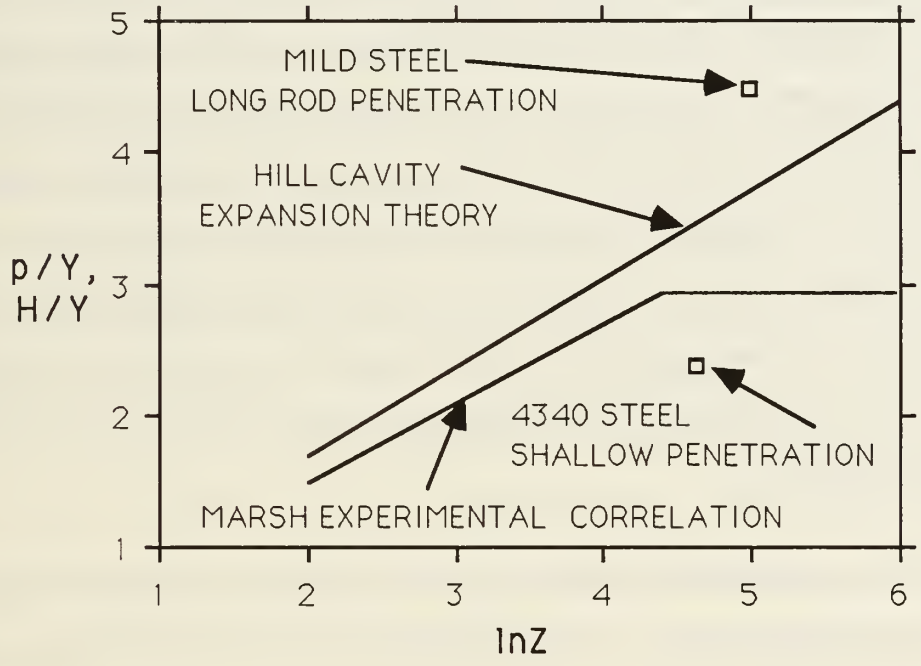

Figure 1. Comparison of Experiment and Theory for the Target Strength Term R_t.

The curve marked Hill cavity expansion theory gives the ratio of the cavity pressure to yield strength, p/Y (for ν=.25). Marsh's correlation of indentation measurements gives the ratio of the hardness to the yield strength, H/Y for ductile materials. The two experimental points are measured ratios of R_t to the dynamic yield strength Y_D and are given in Table I.

Above lnZ = 4.3, the ratio H/Y in Marsh's experiments was a constant. Marsh interpreted these results to mean that the indentation mode changed at lnZ = 4.3 from the radial expansion mode to the plastic flow expected for a rigid-plastic material. Presumably,

above lnZ = 4.3 the rigid-plastic flow requires less work for penetration of a Vicker's indenter than the cavity expansion mode. The elasticity of the material is clearly important for lnZ < 4.3, since the magnitude of Z is proportional to Youngs Modulus E. Poisson's ratio for the material has a much smaller effect on the results since the range of variation for Poisson's ratio is limited.

Several authors have sought to improve the theoretical representation of indentation still making use of Hill's spherical-cavity expansion solution [20,21], but introducing various assumptions about the stress field between the indenter surface and the region of spherical expansion. Some success was achieved in accounting for the effect of indenter geometry, but these analyses did not account for the effect of the free surface. Chiang et al [22] have developed an alternative approach, also based on Hill's spherical expansion theory, which accounts for the effect of the reduced constraint of the free surface on the stress field. This theory agrees well with the experimental data for H/Y (where lnZ<4.3) and is in good agreement with the experimental results on the extent of the plastic zone under the indentation.

Then depending on whether we have deep or shallow penetration at high velocity, the target strength term R_t is set equal to either the pressure p or H where the dynamic yield strength has been substituted for the static yield strength in setting the magnitudes of p and H. The yield strength of some metals such as many aluminum alloys is relatively insensitive to strain rate, whereas the yield strength of low carbon steel increases markedly with strain rate. The dynamic yield strength Y_D for each material can be calculated using the measured values of the Hugoniot Elastic Limits (HELs) where

$$Y_D = \frac{1-2\nu}{1-\nu} HEL$$

Furthermore, if Fig. 1 is used as the basis for predicting the magnitude of R_t observed in impact measurements in metals, it is evident that the value of R_t found for a material is not simply a characteristic property of the target material, but also depends on the type of experiments. Significantly different penetration conditions are represented by the experiments of Tate and Donaldson. Tate measured the performance of mild steel rods with length to diameter ratios of from 5 to 10 , penetrating in mild steel targets at velocities up to 7700 ft/sec. The experiments represent deep penetration so that the spherical expansion theory of Hill should be the appropriate analogy. Donaldson used tungsten carbide spheres impacting in various metals at velocities up to about 5000 ft/sec. Even at the top velocity, the maximum penetration was only 1.4d (where d was the diameter of the sphere) so that a major portion of the deceleration force was generated at relatively shallow penetration. Consequently, the effect of the free surface on the resistance to penetration should have been a factor and Marsh's correlation should be a better guide to the results than the spherical expansion theory. The necessary dynamic data are available for mild steel and 4340 steel. Values of the parameter lnZ, computed for each of these two materials, are listed in Table I. The values of R_t/Y_D found in the two different types of impact experiments are plotted in Fig. 1 and are in general accord with the "predictions" provided by the Hill theory and the Marsh correlation. Close agreement cannot be expected, if for no other reason than the uncertainty in the experimental values. Thus in the case of the long rod experiments, the ratio of R_t/Y_D found in individual experiments varied from substantially less than 4 to more than 5. These results support the view that indentation measurements and the cavity expansion theory are a useful guide to the resistance to high velocity penetration.

B. Brittle Materials

Indentation in brittle materials is complicated by various types of tensile target fracture which depend on the shape and size of the indenter as well as on the properties of

TABLE I. EXPERIMENTAL VALUES FOR THE RATIO OF THE TARGET STRENGTH TERM R_T TO THE DYNAMIC YIELD STRENGTH Y_D.

Materials	HEL (kbars)	lnZ	Y_D (kbars)	R_t/Y_D
4340 R50	22	4.64	13.9	2.37
Mild steel	10.7	5.00	6.5	4.5

where $Z \approx \left(\frac{3}{4+\nu}\right)\frac{E}{Y_D}$

the target. [23] Nevertheless, the general nature of indentation in brittle materials using small radius spherical indenters or sharp blunt indenters, such as the Vicker's indenter, is similar to indentation in ductile materials. Specifically, there is a zone surrounding the indentation where the compressive elastic strength of the target material has been exceeded similar to the plastic zone surrounding indentation in metals. The tensile cracks form predominantly outside of the plastic zone. Surface traces of radial cracks are usually observed emanating from the corners of the Vicker's indenter. The theoretical representation of the zone immediately under the indenter as a "plastic" zone leads to stress fields that are consistent with the formation of tensile cracks during indentation.

Clearly this is not a plastic zone in the usual sense. Most ceramics are restricted in the number of independent slip planes that can be activated particularly at room temperature and the von Mises condition of five independent slip planes for general plastic deformation [24] is not generally satisfied. Even where the required number of independent slip planes can be activated, only limited slip is possible because the slip

systems generally cannot interpenetrate. Consequently the extensive deformation needed to accommodate the large strains near the indenter is generally not possible by dislocation movements alone. Thus the major shear bands observed for indentation in silicon have been attributed to block slip where the theoretical shear strength is exceeded locally [25]. In other materials extensive microcracking has been observed in the plastic zone [26] in addition to evidence of slip flow. In polycrystalline materials large slip would be expected to involve material failure and microcracking at grain boundaries in addition to slip and/or microcracking in grains. Since the indentation pressure is controlled by the pressure that must be generated in the target to allow general deformation under the indenter, the boundary of the "plastic" zone would then represent the compressive stress level required to produce shear failure of the material. Limited slip can occur at stresses below the stress for compressive failure, so there should be some evidence of plastic flow outside of the highly deformed "plastic" zone.

Chiang et al [22] compared experimental measurements (for a few brittle materials) of the radius of the "plastic" zone to the radius of the zone predicted by Hills' spherical expansion theory. Good agreement was found although it is difficult to accurately determine the edge of the plastic zone. A direct comparison of the results of microhardness measurements in ceramics and ductile materials has so far not been done because of the difficulty in measuring the compressive strength of ceramics. Great care must be taken to avoid the presence of applied tensile stresses. [27] The basic problem is that ceramics are much stronger in compression than in tension. Even where the experimental arrangement is designed to assure that the applied stress is compressive, local tensile failure may be a factor in determining the failure stress. [28] Axial microcracks may form and, depending on the grain structure, generate local tensile stresses which precipitate the material failure. Whatever the specific failure modes, measured compressive failure strengths appear to be low. This suggests that the compressive failure stress associated with indentation will be

higher than the compressive failure stress measured in uniaxial tests, because material confinement in indentation prevents general tensile failure when compressive stress is applied.

The suggestion that compressive failure of the target material in indentation is determined by the intrinsic strength of the ceramic has other implications. Thus while the measured value of the compressive failure stress of Al_2O_3 in uniaxial tests increases with increasing strain rate [29] (evidently because of its dependence on thermally activated slip processes which are strain rate sensitive), the compressive failure in indentation should not be sensitive to strain rate. Shock wave measurements where the material is effectively confined laterally and a triaxial state of stress exists should then provide a valid indication of the compressive failure stress levels governing the indentation process.

One limitation in using shock wave measurements is that there is considerable scatter in the measured values of HEL for many ceramics as reported by the same investigator (much of this variation is believed to be due to variations in material properties [30]) and between investigators. Another complication is stress relaxation [31] observed in the measurement of the HEL for some of these ceramics. The elastic shock amplitude decreases with propagation path length. This behavior has been attributed to non-equilibrium effects where it is assumed that the instantaneous shear stress in the shocked material can be higher than the true elastic limit before the material has had time to yield. As yielding occurs, the magnitude of the propagating elastic ware is reduced to the equilibrium value for the HEL. Where such variations of the elastic wave strength as a function of path length have been observed experimentally, the "equilibrium" value for the HEL has been chosen for these computations. Table II shows the experimental HEL values, [30,32-34] the dynamic yield Y_D calculated from these values, and microhardness measurements for a variety of brittle materials. Also shown for comparison are some values of the uniaxial compressive stress σ_c using the technique of Ref. 25 for several hard

ceramics. [35] A measurement at a moderately high strain rate of 10^3 (sec^{-1}) for Al_2O_3 Lucalox is also shown. It seems evident that, despite the improvement in the technique for measuring uniaxial compressive stress, the values measured are still low compared to the compressive failure stress in shock wave measurements.

TABLE II. MECHANICAL PROPERTIES AND THE RESULTING RATIO OF THE HARDNESS H TO THE DYNAMIC YIELD Y_D AS A FUNCTION OF THE PARAMETER Z.

Materials	E (kbars)	H (kbars)	HEL (kbars)	Y_D (kbars)	σ_c (kbars)	$\frac{H}{Y_D}$	lnZ
KT SiC	3650	186	80 ±30	65 ±24	52	2.86	3.7
TiB_2	4820	230	86 ±30	76 ±26	57	3.03	3.84
Al_2O_3 (high density)	3990	196	92	65	38	3.01	4.12
B_4C	4570	274	137 ±4	101	28	2.71	3.4
BeO	3410	123	74	55		2.15	3.78
MgO	3100	92	35	26		3.5	4.44
Fused silica	720	194	98	79		2.45	1.8

Glasses are a special problem because it has been shown that the measured hardness values at room temperature are time dependent. [36] Measurements made at liquid nitrogen temperatures were found to be time independent. Very short time measurements approached these low temperature values whereas long time measurements tended to a lower limit, which in the case of silica was a factor of 3 lower. This behavior is

analogous to static fatigue in glasses where strength is sensitive to load duration. The appropriate hardness value for fused silica consistent with the yield strength derived from the HEL is the value measured at liquid nitrogen temperatures, which is the value entered in Table II.

The ratios of H/Y_D for this group of ceramics are plotted in Fig. 2, where they are compared with the correlation of indentation measurements found for ductile materials by Marsh.[7] With the single exception of BeO, all of the points lie above the Marsh correlation although the trend with the parameter lnZ appears to be similar to the trend found by Marsh. (These remarks have to be qualified by the reminder that there are large uncertainties in the measured values of the HEL for some of the materials). Why should the values of H/Y_D be higher than the Marsh correlation?

At this point it is only possible to speculate about the factors that might modify the ratios of H/Y_D for ceramics as compared to those found for ductile materials. These factors could either increase or decrease the ratio H/Y_D.

a) If the material in the "plastic" zone is microfractured, it seem plausible to associate this microfracture with a decrease of shear strength. According to Hill's theory, that would decrease the pressure required for cavity expansion just as an increase in shear strength due to strain hardening increases the required pressure.

b) Density variations in the "plastic" zone could produce a significant variation in the measured hardness by either contributing to or subtracting from the volume needed for penetration of the indenter. For most ceramics, the volume of the plastic zone is many times larger than the indentation volume. Table III lists the volume ratios predicted by Hill's theory for the ceramics of interest here. Except for fused silica, where the predicted

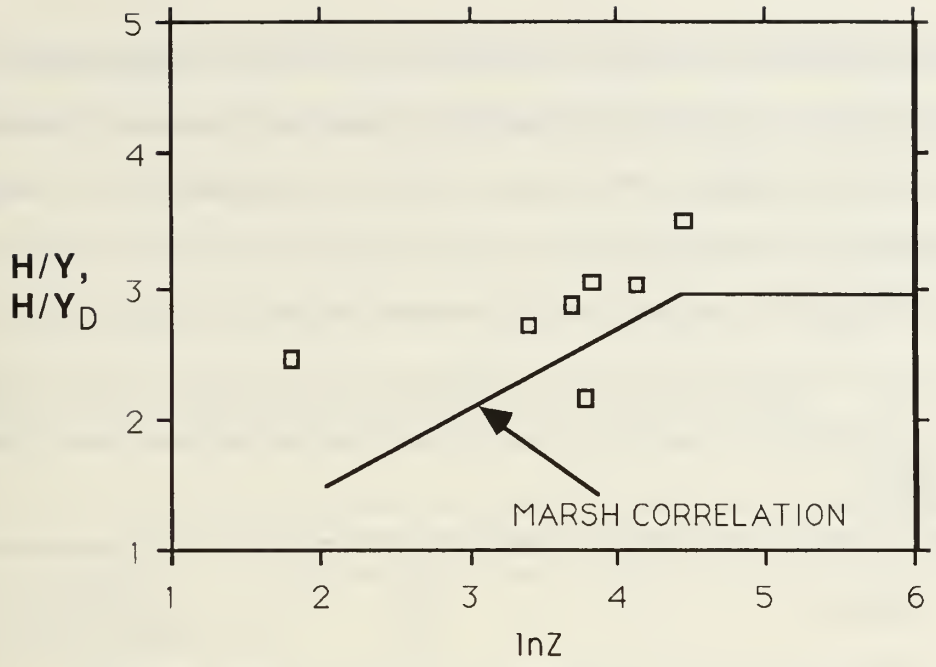

Figure 2. Comparison of the Ratio of Hardness H to Yield Strength Y for Ceramics and Ductile Materials (Given by the Marsh Correlation).

The points shown are the values of the ratio for a range of ceramics (see Table II) where the compressive yield strength used in the ratio is set equal to the dynamic yield strength Y_D.

ratio is only 2.7, density changes in the plastic zone clearly have a large leverage on the resulting indentation volume, so that small density changes can be significant.

If the density in the "plastic" zone increases during penetration, penetration will be easier and the measured hardness will decrease. Two of the materials in the Table, SiC and BeO have a significant initial void fraction, 4% and 5.5% respectively. As microfracture develops above the elastic limit compaction of the failed material may occur. On the other hand fused silica which does not have a significant initial void fraction is permanently densified at pressures above the elastic limit as demonstrated in uniaxial compression tests and shock wave experiments. [37]

Alternatively, the density in the plastic zone can, in principle, be decreased by the generation of voids as the material is strained above the elastic limit thereby increasing the

measured hardness. Since brittle materials are not able to undergo general plastic deformation, when a polycrystalline material is strained above the elastic limit the plastic deformation of the randomly oriented grains cannot be compatible and voids must develop where none existed initially. [38] Also after grain fracture occurs the fractured material would not "fit together" and voids would be expected to persist to high pressures.

TABLE III. PREDICTIONS OF HILL'S THEORY FOR THE RATIO OF THE "PLASTIC" VOLUME TO THE INDENTATION VOLUME FOR CERAMICS.

Materials	$\frac{E}{Y_D}$	$\frac{\text{"Plastic" volume}}{\text{Indentation volume}}$
SiC	56.2	21
TiB_2	63.4	23
Al_2O_3 (high density)	61.4	26
B_4C	45.2	17
BeO	62	25
Fused Silica	9.1	2.7
MgO	119	49

c) Finally, the pressure required for indentation is a measure of the work done on the target material. Where microfracture is present work must be done to fracture the target material in the plastic zone and that should lead to an increase in the required indentation pressure.

In summary, the ratios of H/Y_D for ceramics would be expected to deviate from the correlation curve for ductile materials depending on the particular material behavior in indentation. At the same time, the results shown in Fig. 2 display the general type of behavior expected from cavity expansion theory. The next step will be to examine the connection between these hardness measurements in ceramics and the target resistance to high velocity impact. But first, since the material properties of the targets in the "plastic " zone in indentation can affect the measured hardness, it is desirable to review what is known about the properties of target materials under dynamic conditions, at comparable pressure levels above the HEL, and how these properties compare with the material characterization in indentation.

In dynamic impact there will be a large zone in the target material extending to the projectile interface in which the compressive pressures have exceeded the HEL for the target material. The outer part of this zone where the target material is first being set in motion corresponds to the conditions in the "plastic" zone in indentation. Much higher pressures may be reached between there and the projectile interface. Shock wave measurements indicate a significant loss of shear strength above the HEL for most brittle materials. This loss in shear strength has in some cases been attributed to microfracture of the target material and in other cases to heterogeneous yielding with localized melting. One experimental method for determining the loss of shear strength is to use the displacement of the Hugoniot above the calculated hydrostat as a measure of the residual shear strength. Solids behave elastically in shock compression up to the HEL. Above the HEL, the shear stress is constant at its maximum value given by

$$\tau_{max} = \frac{1}{2} \frac{1-2\nu}{1-\nu} HEL$$

and the offset between the Hugoniot and the hydrostat at the HEL is equal to 4/3 τ_{max} (or 2/3Y, the uniaxial yield stress). [39] On unloading, the stress-strain curve follows a

trajectory displaced below the hydrostat by 2/3Y . For a metal that strain hardens, the offset increases at pressures above the HEL.

When a number of single crystal ceramics, such as sapphire, are exposed to shock waves, they appear to fracture at stresses approaching the theoretical shear strength of the crystal, depending on the crystal orientation. [40] When this happens there is a sharp decrease in the offset of the Hugoniot above the hydrostat. Different values of the HEL are reached (for different crystal orientations) but the Hugoniot data collapse onto a single curve above the HEL which, in the case of sapphire, appears to have a small but definite offset from the calculated hydrostat. It is not clear whether there actually is an offset because, in calculating the hydrostat, it is difficult to account for the void fraction in the fractured material.

Varied behavior above the HEL has been found for polycrystalline ceramic materials such as the ceramics of interest here and no single explanation appears to account for the observations. There is evidence that in brittle materials with low thermal diffusivity, yielding may involve local melting due to the dissipation of elastic shear strain energy, but not all materials exhibit this effect . [6] At shock strengths 2-3 times the HEL, BeO seems to suffer a complete loss of shear strength in the shock wave, whereas alumina appears to retain a substantial fraction of its shear strength above the HEL. [41] However, the work of Munson and Lawrence [42] provides clear evidence that above the HEL, alumina is undergoing progressive microfracture. As the material is taken to higher and higher shock pressures the unloading curves approach closer and closer to the hydrostat, indicating that progressive fracture has occurred during compression and that there is an increasing loss of shear strength. The lack of spall strength in the alumina experiments provides strong evidence that the material is fractured even if it appears to display an effective shear strength under pressure.

It seems reasonable to expect a loss of shear strength in many target materials that have been stressed above the HEL in dynamic impact just as a loss of shear strength would be expected for the "plastic" region in indentation although the amount of the loss may vary from material to material. And it seems reasonable to expect an associated loss of tensile strength in this microcracked material.

IV. THE ROLE OF FRACTURE TOUGHNESS.

Fig. 2 shows that hardness values of ceramics follow a pattern similar to that for ductile materials consistent with the view that cavity expansion theory underlies indentation in both ceramics and ductile materials. It then seems reasonable to postulate that the hardness of a ceramic should be a direct measure of the target strength in high velocity impact. The values of Y_D and in the representation of indentation in ceramics are already derived from shock wave measurements so that the hardness values would then equate directly to the magnitude of the strength term in the analytic representation of impact. As shown in Table II, according to the above postulate the ceramics listed should be capable of providing many times more resistance to penetration than steel, with B_4C and TiB_2 providing the maximum resistance. Table IV lists a number of ceramics where values of R_t ($\rho_t E_*$) have been obtained by the Aeronautical Research Associates of Princeton from impact tests with tungsten carbide spheres. [43] As noted previously, the magnitude of R_t observed in the impact tests was found to vary with the degree of confinement of the target. The maximum values of R_t were obtained when the target was strongly confined and are the values listed in the Table. All of the ceramics have higher values of R_t than 4340 steel, but the levels of R_t are much lower than the levels expected on the basis of the indentation hardness measurements since R_t/H ranges from .17 to .30 well below unity. What property of the targets can account for this result?

TABLE IV. CORRELATION OF THE RATIO OF THE TARGET STRENGTH R_T TO THE HARDNESS H WITH THE FRACTURE TOUGHNESS K_{IC}.

Materials	H (kbars)	R_t (kbars)	$\frac{R_t}{H}$	K_{IC} ($MNm^{-3/2}$)	Y_{eff} (kbars)
KT SiC	186	63	.34	4.9	22
TiB_2	230	87	.38	6.7	29
Al_2O_3 (high density)	196	55	.28	4	18
B_4C	274	52	.19	4 (?)	19
Fused Silica	194	36	.19	.7	15
Si_3N_4	160	48	.30	5	
$MgAl_2O_4$	160	33	.21	1.6	

Two different phenomena can affect the condition of the target. First, as has been discussed, the target material may suffer a major loss of shear strength when subjected to pressures well above the HEL. In the initial moments of impact, high transient pressures are reached. This pressure rapidly drops as the shock wave spreads out in the target. Exposure to these high pressures above the HEL would weaken some small volume of the target before the arrival of the projectile. As the impact velocity is increased, the volume affected would grow. However, Hill's solution for the expansion of a cavity in a solid predicts that the volume of the "plastic" zone will be large compared to the cavity. For the ceramic materials considered here, the radius of the edge of the "plastic" zone is estimated

to be several times the radius of the hole. Consequently the plastic zone that must develop as penetration proceeds should swamp the zone affected by the transient phenomena.

Second, extensive tensile failure of brittle targets is produced by high velocity impact. Numerous cracks propagate into the target at velocities which appear to be determined by the dilatational acoustic velocity in the target. The ratio of the crack velocity to the acoustic velocity depends on the material and ranges from 0.27 for glass to .56 for magnesium oxide. [7] As the impact becomes more severe, centers of secondary crack patterns may be generated ahead of the initial propagating cracks increasing the velocity at which target damage is propagated into the target up to approximately .85 of the acoustic velocity for glass targets and increasing the degree of damage. [44] The final pattern of cracks in the target is also significantly affected by reflections from the boundaries where these reflections can interact with the developing cracks.

The length of the radial cracks appears to be largely governed by the maximum force generated early in the impact. [45] Evans et al used targets with maximum dimensions 50 times the projectile diameters so that boundary reflections did not play a role in the experiments. The length of radial cracks in the targets C_r were found to depend on the fracture toughness of the target K_{IC} (the critical stress intensity factor), as well as the radius R_p and the velocity V of the impacting projectile, where

$$C_r \sim \left[\frac{(R_p V)^2}{K_{IC}} \right]^{\frac{2}{3}}$$

Under the projectile size and impact conditions of the ARAP experiments, the fractured zone of a large target would extend out to approximately ten times the radius of the impacting sphere. However, in the ARAP experiment, the ceramic targets were

generally thin, of the order of the impacting sphere diameter. Therefore the ceramic targets resisting penetration in the experiments are targets that have suffered extensive tensile fracture damage.

The fractured target must be confined to keep it from flying apart or from being readily pushed out of the way by the penetrator. Subsequent target fracture such as surface spalling may occur on pressure unloading as penetration ceases, but should have little influence on the resistance to penetration of the target. We are led to the following postulate: the more fractured the target, the less resistance it will be able to offer to projectile penetration. According to the correlation for C_r, the ratio C_r/R_p only marginally increases with increasing size of the projectile, but C_r increases more than linearly with velocity. If greater crack length can be taken as an indication of greater target fracture then the target strength terms would be expected to decrease as the velocity of impact increases. It also follow that at a given impact velocity with a specific projectile, increased fracture toughness would reduce the extent of target damage.

If the state of damage is a key parameter in determining the resistance to penetration then other factors besides those already discussed may be important. Higher fracture stresses, σ_f, would release more elastic energy on fracture thereby leading to greater breakup of the target. The state of target damage should then decrease with decreasing values of the parameter σ_f/K_{IC} (see Ref. 24). Unfortunately values of fracture strength in the literature exhibit extensive scatter and are known to be highly dependent on the methods of fabrication and the microstructure so it has not been feasible to examine the correlation of data with this parameter. Instead the correlation of target strength with fracture toughness alone, (at the same dynamic conditions), will be examined. The impedance match between the ceramic target and confining material could also affect the state of damage of the target. Shock reflections from the boundaries have been shown to affect the resulting fracture pattern. Finally, the damage to the target will be heaviest near the region of the initial

impact. If the target is thick, long rods may encounter increasing resistances to penetration as they progress through the target.

Values of the fracture toughness for these materials are listed in Table IV. In some cases fracture toughness measurements were available from the supplier of the specific materials used in the impact tests. In other cases fracture toughness values are available in the literature for nominally the same material. The matter is complicated by the fact that the fracture toughness of ceramics also depends on microstructure and fabrication procedures and in many cases supposedly the same but actually different materials have been used for the ballistic tests and the hardness measurements. Table IV also lists the ratio R_t/H, where R_t is the target strength term from the ballistic experiments and H is the measured hardness. The ratio R_t/H is plotted in Fig. 3 as a function of the fracture toughness. With the single exception of B_4C, these data show an increase in the ratio of R_t/H with increasing K_{IC}. But the fracture toughness assigned to B_4C may be too large. The B_4C used in the impact experiments was a Ceradyne product for which no measurements of fracture toughness are available. The value of K_{IC} for B_4C that is shown in the figure is the value reported by Viechnicki et al [35] for B_4C from a different supplier. The B_4C targets in the ballistic tests were extensively fractured [43] which by comparison with the fracture behavior of other materials tested would suggest a much lower value of the fracture toughness.

Two conclusions can be drawn from Fig. 3. First of all, small changes in K_{IC} are not significant. The variation of R_t/H from .19 to .38 corresponds to a factor of 10 change in the fracture toughness. Secondly, if the trend shown is correct, it also indicates that very substantial increases in R_t might be realized if K_{IC} could be increased from say a value of 7 for TiB_2 to perhaps 30 or 40 where a linear extrapolation of the curve would reach $R_t/H=1$. If the breakup of the target on impact can be greatly impeded, it may be possible to better exploit the high hardness of these materials in resisting high velocity penetration.

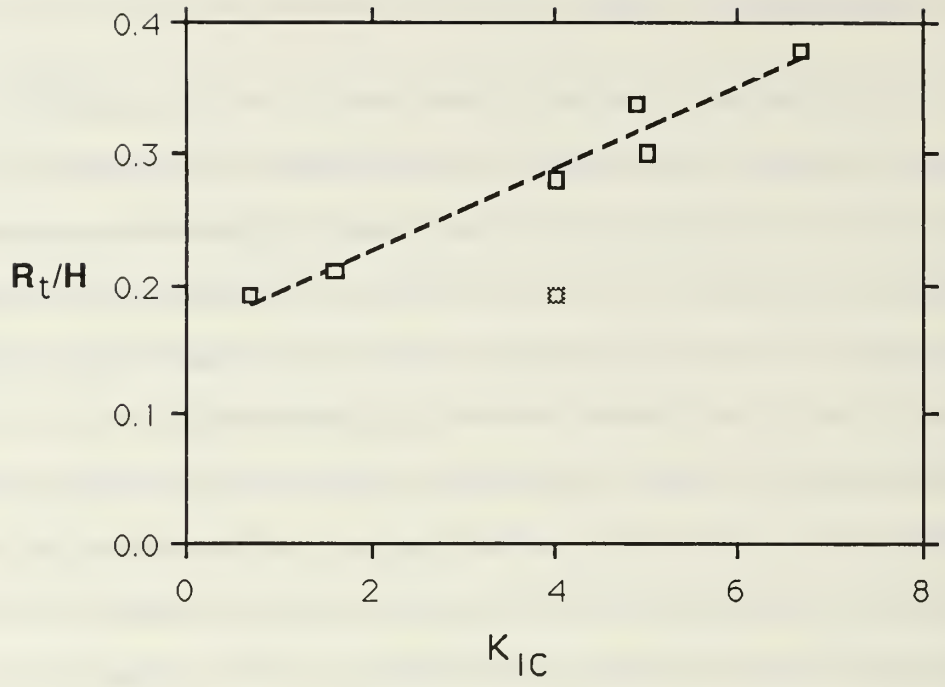

Figure 3. Correlation of the Ratio of the Target Strength Term R_t to the Hardness H with the Fracture Toughness K_{IC} for a Range of Ceramics (see Table IV).

One complication in assessing the potential of composites is the experimental evidence that the work of fracture decreases with increasing strain rate although a limiting value is reached at high rates of impact testing. [46] For some composites, reductions of about 50% have been observed. Apparent difference between fracture modes in laboratory testing and in ballistic testing have also been reported by Viechnicki et al [35] for formulations of TiB_2 and SiC which contained a second phase. The measured fracture toughness of these materials increased when a second phase was added (other material properties such as hardness also changed) apparently due to a shift from transgranular to increased intergranular failure. Viechnicki found a negative correlation between fracture toughness and the ballistic limit for these materials (compared to single phase TiB_2 and SiC), contrary to the positive correlation between fracture toughness and R_t shown in Fig. 3. If the dynamic behavior is substantially different than the static behavior then

measured increases in fracture toughness could be misleading. It is also not clear whether ballistic limits are simply correlated with the parameter R_t.

Unfortunately, low fracture toughness appears to be a basic characteristic of brittle solids with high hardness. Two different approaches have been followed to increase the toughness of ceramics. Toughness can be increased by distributions of particulates (including precipitates) but the increases that have been achieved are not nearly the magnitude desired. However fiber reinforced composites offer the possibility of much larger increases in toughness. Stress intensity values of K_{IC} from $10MNm^{-\frac{3}{2}}$ to $20MNm^{-\frac{3}{2}}$ have been obtained for carbon fiber and silicon fiber reinforced glasses. [46] If the correlation shown in Fig. 3 is valid, and if the increase in fracture toughness is not bought at the expense of a decrease in hardness, then a composite based on silica might well exceed the target strength values for materials such as TiB_2 and SiC. For application to armors such materials would have the added advantage of low weight.

V. CRATER SIZE.

How should the crater size in brittle materials be expected to compare with the crater size in ductile materials? First consider ductile targets. Aside from the transient region at the initial section of the crater, and the bottom of the cavity, the craters are cylindrical. Since the solution for the expansion of a spherical hole in an elastic/plastic solid has proved to be a useful guide to the resistance of targets to high velocity penetration, it is of interest to examine the applicability of Hill's solution for the expansion of a cylindrical cavity to crater formation during high velocity impact. Neglecting strain hardening, the pressure required to expand a cylindrical cavity is given by

$$p = \frac{Y}{\sqrt{3}}\left[1 + \ln\frac{\sqrt{3}E}{(5-4\nu)Y}\right] \tag{5}$$

so that the work required to form the cavity is pV_c, where V_c is the volume of the cavity.

If the material strain hardens, the pressure needed to expand the cavity will be increased since more work must be done on the target material to form the cavity. As applied to crater formation in high velocity impact, dynamic values of the yield strength of the target material should be used.

Hill's theory specifies the size of the cylindrical cavity that can be generated with the least expenditure of energy. In high velocity impact the process of crater formation is less efficient than the slow formation of a cylindrical cavity. Some of the kinetic energy of the projectile is absorbed by the projectile itself as it is deformed by the impact. Other energy is carried away in pressure waves or is lost in heat or other dissipation associated with the very high pressures and velocities of impact. So clearly the crater volume calculated using Hill's theory should be greater than the experimental crater volumes.

The Christman-Gehring (C-G) empirical correlation [9] for the crater volume produced by rods and jets at velocities from 2 km/sec to 10 km/sec has been generally accepted as a useful guide to cratering in metals. However, their correlation was limited to experimental data obtained with two materials; aluminum and steel. The crater volume V_c was given by the following equation

$$V_c \propto \left(\frac{\rho_p}{\rho_t^3}\right)^{\frac{1}{6}} \frac{E_n}{B_{max}}$$

where ρ_p and ρ_t are projectile and target densities respectively, B_{max} is the "maximum hardness as measured on a sectioned target just below the bottom of the crater" and E_n is the kinetic energy of the projectile. The use of B_{max} instead of the Brinell Hardness of the target before impact was intended to account for both strain hardening and the target strength under the high strain rate conditions of impact. No explanation was offered for the

forms of the dependence on ρ_p and ρ_t given by the correlation. When the penetrator and target are of the same material the crater volume varies as $\rho_t^{1/3}$.

It should be noted that according to Hill's theory, the difference in crater size between aluminum and steel targets is primarily due to the difference in dynamic yield strength and Young's modulus between the two materials. Target density does not appear at all. Craters of the same size in materials with markedly different values of E/Y would require significantly different energy for their formation.

The measurements of B_{max} needed for the calculation of V_c are only listed for a few target materials in Ref. 9. Table V lists the crater volume according to C-G for two common aluminum and steel targets. According to Hill's theory, the crater volume $V_c = E_n/p$. This expression for V_c can be compared to C-G if dynamic values are used for the yield strength. Unfortunately, dynamic yield data for the specific metals used by C-G do not appear to be available in the literature, but shock wave measurements of the HEL are available for closely related steel and aluminum alloys, Al 2024-T4 (compared to Al 2024-T3) and 1020 low carbon steel (compared to C1015).

In the case of the steel targets, the crater volume predicted by Hill's theory for the same E_n is only a factor of 1.3 greater than the experimental results. For the aluminum targets the crater volume is a factor of 2.3 greater (see Table V). However, the difference in the dynamic behavior of the two materials would bring the ratios of theory to experiment closer together. The yield point of the 2024 aluminum is insensitive to strain rate, but almost a factor of two increase in flow stress due to strain hardening seems likely, based on static measurements. This would decrease the crater volume predicted by Hill's theory for aluminum and would therefore lower the ratio of the theoretical to experimental crater volumes. At the same time whereas the dynamic yield stress of low carbon steel as shown in the table is more than double the static yield stress, stress relaxation from the initial HEL

TABLE V. COMPARISONS OF THE PREDICTION OF CRATER VOLUME USING THE CHRISTMAN-GEHRING CORRELATION AND HILL'S CYLINDRICAL CAVITY EXPANSION THEORY.

	Brinell Hardness		$\frac{\text{Crater volume (C-G)}}{\text{projectile energy}}$
	B_{max}	$\rho_t^{1/3}B_{max}$	V_c/E_n
Materials	(kg/mm^2)	$(gm^{1/3}/cm)(kg/mm^2)$	(cc/joule)
Al 2024T3	155	215	4.65×10^{-4}
Steel C1015	165	325	3.10×10^{-4}
	HEL (kbars)	Dynamic yield Y_D (kbars)	$\frac{\text{Crater Volume (H)}}{\text{Crater volume (C-G)}}$
Al 2024-T4	5.4	2.8	2.2
Steel 1020	11.4	7.4	1.3

value is observed up to large strains [47] before strain hardening sets in. This would have the effect of increasing the theoretically predicted crater volume for the 1020 steel.

What does the expansion theory say about craters in brittle materials? First of all, according to Hill's theory the pressure required to expand a cylindrical cavity (a multiple of the yield stress) is not much different than the pressure required to expand a spherical cavity. One interpretation that can be drawn from the fact that the target strength terms from ballistic measurements are much lower than the values expected from hardness measurements is that the effective yield stress of fractured ceramics is lower than the yield stress Y_D derived from the HEL for the material. The effective yield stress Y_{eff} can be defined as

$$Y_{eff} = \left(\frac{R_t}{H}\right) Y_D \qquad (6)$$

where values based on the penetration data and available values of Y_D are shown in Table IV. These values of Y_{eff} can then be used to estimate the crater volume applying Hill's theory for the expansion of a cylindrical cavity (equation 5).

The relative crater volumes for this group of ceramics are compared with the crater volume for rolled homogeneous armor (RHA) in Table VI assuming the same kinetic energy of the projectile. Except for fused silica, the crater volumes are predicted to be smaller than the crater volume for RHA. This would be the result if the target material that had been exposed to pressures above the elastic limit retained its cohesion. If not, the microfractured material may be swept away during the impact. According to Hill's theory, the volume of material around the cavity that will have exceeded the elastic limit is large compared to the cavity volume. The ratio of the yield boundary c to the cavity radius a for each ceramic is given by

$$\frac{c}{a} = \left[\frac{2E}{(5-4\nu)Y}\right]^{\frac{1}{2}}.$$

This ratio varies from 4.7 to 10.5 for the ceramics listed in Table VI and is 9.4 for RHA. Consequently as shown in the last column in Table VI, if microfractured material is swept away, the volume of the craters may be many times the volume of the crater in RHA for the same impact conditions.

VI. CONCLUSIONS

It is well known that high velocity penetration of long rods in ductile materials can be represented using a modification of the hydrodynamic theory for shaped charges incorporating strength terms for the penetrator and target. The pressure required to move the target material out of the way in high velocity penetration is related to the pressure

TABLE VI. POSSIBLE CRATER VOLUMES IN CERAMICS COMPARED TO ROLLED HOMOGENEOUS ARMOR.

Material	E/Y_{eff}	$\frac{\text{Crater volume}}{\text{RHA crater volume}}$	$\frac{\text{Plastic volume}}{\text{RHA crater volume}}$
KT SiC	164	.75	41
TiB_2	165	.66	31
Al_2O_3	222	.80	70
B_4C	226	.78	64
Fused Silica	48	1.04	23
RHA	167	1.00	-

required for the slow expansion of a spherical cavity in an infinite medium as given by an early theory developed by Hill. Hill's solution is for an elastic/plastic solid that satisfies the Tresca yield criterion. At a given value of Young's modulus E and Poisson's ratio ν, the pressure required for expansion is a multiple of the material yield stress. The magnitude of the target strength term found in ballistic experiments is a comparable multiple of the yield stress if the dynamic value of the yield stress is used in place of the static value. It has also been shown that the pressure required for indentation in ductile materials is closely related to the pressure required for cavity expansion up to some critical value of E/Y. Below the critical value, Hill's theory provides the basis for the theoretical representation of indentation if the theory is modified to account for the effect of the free surface.

The objective of this investigation was to identify the mechanical properties of ceramics of importance in resisting high velocity penetration. Since indentation in metals has been shown to be closely related to the resistance of metals to high velocity penetration, the first step was to explore the possibility that indentation in ceramics would be similarly related to high velocity penetration.

Important new phenomena are observed in the indentation of ceramics. Nevertheless, if sharp or small radius indenters are used, indentation in ceramics exhibits features observed in indentation in metals. There is a sizeable zone under the indenter where the material has exceeded the elastic limit, similar in extent to the plastic zone in indentation in metals. Depending on the material, the zone may be characterized by slip bands, microcracking, and densification or void generation although the extent of plastic flow that is possible along slip is generally limited.

In this paper, indentation measurements in ceramics are compared to the correlation as a function E/Y found for ductile materials. Measurements of the Hugoniot Elastic Limits are used to determine the compressive yield stress of the material. Since only limited slip flow is possible in these materials, this stress will correspond to the stress required for shear failure for the ceramics, which under the confined conditions of indentation should be governed by the intrinsic strength of the ceramics, not by the flow stress for slip flow. For those materials where data are available, the resulting ratios of indentation pressure to elastic limit are generally larger than the equivalent ratio for ductile materials at the same value of E/Y (with one exception) but the variation with E/Y is comparable. Because of the differences in behavior of ductile and brittle materials, there is no reason to expect the ratios of H/Y to be identical. It is possible that the primary reason the ratio is larger for ceramics is because of the work that goes into generating slip bands or microcracking the ceramic.

Based on the general similarity of the indentation phenomena for both ductile and brittle materials, we might plausibly expect the target strength term for ceramics, as found in ballistic experiments, to be given by the hardness, as is true for metals. This is clearly not the case. The observed target strength terms are lower than would be expected on this basis by a factor of 2.5 to 5.

It is postulated that the target strength is lower than might be expected because penetration takes place in a weakened target. Target fracture is generated in the initial stages of impact, propagating ahead of the penetrator. The more fractured the target, the lower the material resistance. No single parameter determines the state of the target. For a thick target, the target damage produced at impact will not be uniformly distributed throughout the depth of the target. Target fracture is known to increase with increasing velocity. As far as material properties are concerned, impact data are available that show decreasing fracture of the target with increasing fracture toughness. A new interpretation of the available ballistic data leads to the conclusion that the resistance to penetration increases with increasing fracture toughness of the target. The key performance parameter is the ratio of the strength term R_t, as determined from the ballistic experiments to the hardness H. Based on experimental data for shallow penetrations at a velocity of 5000 ft/sec, this ratio shows an increase with increasing fracture toughness for most of the ceramics tested. Using this correlation to extrapolate to $R_t/H \approx 1$, (where the target would no longer be significantly weakened by fracture) the fracture toughness K_{IC} would have to be increased to 25 - 30$MNm^{-\frac{3}{2}}$ to exploit fully the hardness of ceramics at this velocity. It has been reported that the fracture toughness of ceramics can be substantially increased by fiber reinforcement up to $K_{IC}=20MNm^{-\frac{3}{2}}$ for reinforced glasses. The application of fiber reinforcement to inherently hard ceramics may improve the already good resistance of ceramics to penetration.

Because ceramics offer more resistance to penetration than metals it might be expected that smaller craters would be formed. The ratio R_t/H for each ceramic (at a velocity of 5000 ft/sec) is used to define an effective yield stress for a fractured target from which crater size can be estimated. However, the ceramic materials in the vicinity of the penetrator, exposed to pressures well above the HEL, are likely to be extensively microcracked creating a rubble that may be swept away during penetration thereby greatly increasing the crater size.

REFERENCES

1. Graham F. Silsby, "Penetration of Semi-Infinite Steel Targets by Tungsten Long Rods at 1.3 to 4.5 km/sec," Eight International Symposium on Ballistics, Orlando, Florida, p. TB-31, Oct (1984).

2. W. A. Allen, and J. W. Rogers, J. Franklin Inst., 275, (1961).

3. Alekseevskii, Fizika Gorenirza i Vzryva, Vol. 2, 99, 1966.

4. Tate, J. Mech. Phys. Solids, Vol. 15, 387, (1967).

5. C. duP. Donaldson, R. Contiliano and C. V. Swanson, "The Qualification of Target Materials Using the Integral Theory of Impact", Aeronautical Research Associates of Princeton (ARAP), Report 295, (Dec. 1976).

6. L. Davison and R. A. Graham, "Shock Compression of Solids," Physics Reports Vol. 55, No. 4, 255-379, (1979).

7. J. E. Field, Contemp. Phys. Vol. 12, No. 1, 1, (1971).

8. R. M. Contiliano, T. B. McDonough, & C. V. Swanson, "Application of the Integral Theory of Impact to the Qualification of Materials and the Development of a Simplified Rod Penetration Model", ARAP Report 368, (1978).

9. D. R. Christman and J. W. Gehring, J. Appl. Phys., Vol. 37, No. 4, 1579, (1966).

10. R. J. Eichelberger, J. Appl. Phys., Vol. 27, No. 1, 63, (1956).

11. R. F. Bishop, R. Hill, and N. F. Mott, Proc. Phys. Soc., London, Vol. 57, Part 3, 147, (1945).

12. D. S. Haugstad, D. S. Dullum, J. Appl. Phys., Vol. 52, No. 8, 5066, (1981).

13. T. W. Wright, "Penetration with Long Rods: A Theoretical Framework and Comparison with Instrumented Impact." Ballistic Research Laboratory Report, ARBRL-TR-02323, (1981)

14. M. E. Backman, S. A. Finnegan, and K. G. Whitham, "The Formation of Stagnation Zones in Stable Penetrations of Brittle Materials," Sixth International Symposium on Ballistics, Orlando, Florida, pp. 494-501, (1981).

15. W. D. Hayes and R. F. Probstein, Hypersonic Flow Theory, (Academic Press, New York), p. 70, (1959).

16. J. Sternberg, "A Critical Review of Target Strength Effects in Resisting High Velocity Penetration," R&D Associates Report, TR-188900-001, (1985).

17. R. Hill, The Mathematical Theory of Plasticity, (Oxford University Press, Oxford), (1950).

18. H. G. Hopkins, "Dynamic Expansion of Spherical Cavities in Metals," Progress in Solid Mechanisms, Vol. 1, (North Holland, Amsterdam), pp. 83-164, (1960).

19. D. M. Marsh, Proc. R. Soc., London, Sect. A, Vol. 279, 420, (1964).

20. K. L. Johnson, J. Mech. Phys. Solids, Vol. 18, 115, (1970).

21. E. J. Studman, M. A. Moore, S. E. Jones, J. Phys. D, Vol. 10, 949 (1977).

22. S. S. Chiang, D. B. Marshall, D. B., and A. G.Evans, J. Appl. Phys. Vol. 53 (l), 298, (1982).

23. Lawn and Wilshaw, J. Mat. Sci. 10, 1049, (1975) .

24. R. W. Davidge, Mechanical Behavior of Ceramics, (Cambridge University Press, Cambridge), 1979, p. 61.)

25. M. J. Hill and D. J. Rowcliffe, J. Mater. Sci, Vol. 9, 1569, (1974).

26. A. G. Evans and T. R. Wilshaw, Acta Metall, Vol. 24, 939, (1976).

27. C. A. Tracy, J. Testing and Evaluation, Vol. 15, No. 1, 14, (1987).

28. J. Lankford, J. Mater. Sci, Vol. 16, 1567, (1981).

29. J. Lankford, Fracture Mechanics of Ceramics, Vol. 3, (Plenum Press, NY), pp. 245-56, (1978).

30. W. H. Gust, A. C. Holt, and E. B. Royce, J. Appl. Physics, Vol. 44, No. 2, (1973).

31. C. E. Duvall, Stress Waves in Anelastic Solids, edited by H. Kolsky and W. Prager, (Springer-Verlag, Berlin), p. 20-32, (1964).

32. W. H. Gust and E. B. Royce, J. Appl. Phys., Vol. 42, No. 1, 276 (1971).

33. J. Wackerle, J. Appl. Phys., Vol. 33, No. 3, 922 (1962).

34. L. D. Meier, and T. J. Ahrens, J. Geophys. Res. Vol. 82, No. 17, 2523, (1977).

35. D. Viechnicki, W. Blumenthal, M. Slavin, C. Tracy, and H. Skeele, Pressented at Third TACOM Armor Coordinating Conference, 17-19 Feb. 1987, Monterey, California.

36. D. M. Marsh, Proc. Roy. Soc. A, 282, 33, (1965).

37. J. Arndt, U. Hornemann, and W. F. Müller, Phys. Chem. Glasses, Vol. 12, No. 1, 1, (1971).

38. G. W. Groves and A. Kelly, Phil. Mag., Vol. 8, p. 877, (1963).

39. G. R. Fowles, J. Appl. Phys., Vol. 32, No. 18, 1475, (1961).

40. R. A. Graham and W. P. Brooks, J. Phys. Chem. Solids, Vol. 32, 2311 (1971).

41. T. J. Ahrens, W. H. Gust, and E. B. Royce, J. Appl. Phys., Vol. 39, No. 10, 4610, (1968).

42. D. E. Munson and R. J. Lawrence, J. Appl. Phys., Vol. 50, No. 10, 6272, (1979).

43. W. Snowden, Defense Sciences Division, DARPA, April 30, 1985, private communication.

44. V. Hornemann, H. Rothenhausler, and H. Senf, Paper presented at 3rd Conf. Mech Prop. High Rates of Strain, Oxford, (1984).

45. A. G. Evans, M. E. Gulden, and M. Rosenblatt, Proc. R. Soc. London, A, 361, (1978).

46. D. C. Phillips, Fabrication of Composites (North-Holland; Amsterdam), "Fiber Reinforced Ceramics," 378-428, (1983).

47. O. E. Jones, F. W. Neilson, and W. B. Benedick, J. Appl. Phys., Vol. 33, No. 11, 3224, (1962).

INITIAL DISTRIBUTION LIST

	Copies
Director of Research Administration (Code 012) Naval Postgraduate School Monterey, CA 93943-5000	1
Defense Technical Information Center Cameron Station Alexandria, VA 22314	2
Library (Code 0142) Naval Postgraduate School Monterey, CA 93943-5000	2
Joseph Sternberg Code 73 Naval Postgraduate School Monterey, CA 93943-5002	15